Published in final edited form as:
Cell Rep. 2014 April 24; 7(2): 412–423. doi:10.1016/j.celrep.2014.03.025.

Folliculin Controls Lung Alveolar Enlargement and Epithelial Cell Survival through E-cadherin, LKB1 and AMPK

Elena A. Goncharova[1,5], **Dmitry A. Goncharov**[1,5], **Melane L. James**[1], **Elena N. Atochina-Vasserman**[1], **Victoria Stepanova**[2], **Seung-Beom Hong**[1], **Hua Li**[1], **Linda Gonzales**[4], **Masaya Baba**[6], **W. Marston Linehan**[6], **Andrew J. Gow**[5], **Susan Margulies**[3], **Susan Guttentag**[4], **Laura S. Schmidt**[6,7], and **Vera P. Krymskaya**[1,*]

[1]Pulmonary, Allergy and Critical Care Division, Airways Biology Initiative, Department of Medicine, University of Pennsylvania, Philadelphia, PA 19104

[2]Department of Pathology and Laboratory Medicine, Perelman School of Medicine, University of Pennsylvania, Philadelphia, PA 19104

[3]Department of Bioengineering, School of Engineering and Applied Science, University of Pennsylvania, [3]Children's Hospital of Philadelphia, Philadelphia, PA 19104

[4]Vascular Medicine Institute, University of Pittsburgh, Pittsburgh, PA 15261

[5]Department of Pharmacology & Toxicology, Rutgers University, Piscataway, NJ 08854

[6]Urologic Oncology Branch, National Cancer Institute, Bethesda, MD 20892

[7]Basic Science Program, Leidos Biomedical Research, Inc., Frederick National Laboratory for Cancer Research, Frederick, MD 20892 USA

Summary

Spontaneous pneumothoraces due to lung cyst rupture afflict patients with the rare disease Birt-Hogg-Dubé (BHD) syndrome caused by mutations of the tumor suppressor gene *folliculin* (*FLCN*) by unknown mechanism. BHD lungs exhibit increased alveolar epithelial cell apoptosis. We show that *Flcn* deletion in lung epithelium leads to cell apoptosis, alveolar enlargement and impaired lung function. FLCN loss also impairs alveolar epithelial barrier function. *Flcn*-null epithelial cell apoptosis is the result of impaired AMPK activation and increased cleaved caspase-3. AMPK activator LKB1 and E-cadherin are downregulated by *Flcn* loss and restored by its expression. Flcn-null cell survival is rescued by AICAR or constitutively active AMPK. AICAR also improves lung condition of $Flcn^{f/f}$*:SP-C-Cre* mice. Our data show that Flcn regulates lung epithelial cell survival and alveolar size and suggest that lung cysts in BHD may result from an underlying defect in alveolar epithelial cell survival attributable to FLCN regulation of the E-cadherin-LKB1-AMPK axis.

*Correspondence to: Vera P. Krymskaya, Ph.D., M.B.A., University of Pennsylvania, Translational Research Laboratories, 125 South 31St Street, Room 1213, Philadelphia, PA 19104, USA, Phone: (215) 573-9861, krymskay@mail.med.upenn.edu.

Introduction

Birt-Hogg-Dube (BHD) syndrome is a rare autosomal dominant disorder that affects lung, skin and kidney (Birt et al., 1977). In the lung, 80–100% of patients with BHD develop multiple thin-wall cysts without evidence of neoplasia, inflammation, or fibrosis (Gupta et al., 2013). Cyst rupture and lung collapse cause spontaneous and recurrent pneumothoraces (Gupta et al., 2013). In contrast to lung, *FLCN* mutations in the kidney result in bilateral multifocal renal cell carcinomas (Schmidt, 2004), and in hair follicles result in hamartomas (fibrofolliculomas). The mechanism by which the loss of FLCN promotes the development of cysts but not neoplasia is unknown.

Genetic mapping in families with BHD identified the *Folliculin* (*FLCN)* gene locus (Nickerson et al., 2002; Schmidt et al., 2001). Loss of heterozygosity in BHD lesions supports a tumor suppressor function for *FLCN* (Vocke et al., 2005). Homozygous $Flcn^{-/-}$ mice are embryonically lethal, and heterozygous $Flcn^{+/-}$ mice develop kidney tumors without lung pathology (Hasumi et al., 2009). In *Drosophila* and yeast, FLCN is involved in the mTOR signaling pathway and in energy metabolism (Liu et al., 2013; van Slegtenhorst et al., 2007). Inactivation of FLCN induces mitochondrial gene expression (Hasumi et al., 2012). Studies also suggest crosstalk of FLCN with the master energy sensor AMP-activated protein kinase (AMPK) via FLCN-interacting proteins FNIP1 and FNIP2 (Baba et al., 2006; Hasumi et al., 2008; Takagi et al., 2008). How these signaling events relate to FLCN function in normal lung or in pulmonary cyst development in BHD is unknown.

The prevailing hypothesis used to explain the development of emphysematous alveolar enlargement and cyst formation in lung diseases involves an imbalance between matrix degrading matrix metalloproteinases (MMPs) and their endogenous inhibitors tissue inhibitor of metalloproteinases (Shapiro and Ingenito, 2005; Suki et al., 2003). The notion, however, that alveolar epithelial cell apoptosis is a primary event in the pathogenesis of alveolar enlargement related to lung injury has become an area of significant interest (Henson and Tuder, 2008; Mouded et al., 2009). The FLCN-dependent mechanism of cystic lung enlargement in BHD and the functional significance of *FLCN* inactivation in the lung remain uncharacterized.

Cell-cell and cell-matrix interactions are critical components of epithelial cell survival, and disruption of these interactions often leads to caspase-mediated apoptosis (Frisch and Screaton, 2001). AMPK is required for cell survival and for the maintenance of epithelial cell junctions (Hardie, 2011; Lee et al., 2008; Liu et al., 2010; Mirouse et al., 2007; Zheng and Cantley, 2007). AMPK activity is regulated through phosphorylation by LKB1 (Hardie, 2011), a tumor suppressor gene associated with 30% of lung cancers (Makowski and Hayes, 2008). LKB1 controls the maturation of apical junctions in human bronchial epithelial cells (Xu et al., 2013). E-cadherin regulates the localization of LKB1 to epithelial cell junctions, and loss of E-cadherin impairs LKB1-mediated AMPK activation (Sebbagh et al., 2009).

These observations raise the possibility that FLCN might be involved in the regulation of AMPK signaling in alveolar epithelial cells (AECs) and that inactivating mutation of *FLCN*

might impair epithelial cell junctions and cell survival. In this study, we investigate this possibility with cell-type specific inducible *Flcn* deletion in mouse lung epithelium and with *FLCN*-null human and mouse epithelial cell systems.

Results

Loss of *Flcn* in lung epithelium results in increased alveoli

H&E staining of control human lung reveals typical lung structure (Figure 1A, left panel). In contrast, lungs from BHD patients showed irregular and disrupted lung parenchyma (Figure 1A, right panel). Healthy alveoli are lined with type I and the surfactant protein-C (SP-C)-expressing type II AECs (Figure S1A–B), a renewable population of progenitors in these distal airspaces. We used co-immunostaining to determine FLCN expression in human lung from healthy controls and BHD subjects. In control lung, FLCN staining co-localizes with SP-C expression in AECs (Figure 1B, upper panels). Co-immunostaining of lung tissue from BHD patients detect very little FLCN in alveolar SP-C-positive cells (Figure 1B, lower panels).

To evaluate the role of FLCN in lung, we selectively deleted *Flcn* in SP-C-expressing alveolar epithelial type II cells (*Flcn*$^{f/f}$*:SP-C-Cre)* by crossing *Flcn*$^{f/f}$ mice (Baba et al., 2008) with *SP-C-rtTA/tetO-Cre* (line 2) mice (Perl et al., 2009) (Figure S1C) to generate *Flcn*$^{f/f}$*:SP-C-Cre* mice with inducible *Flcn* deletion in SP-C-expressing cells by a dietary supplementation with doxycycline starting at 6 weeks of age. Under this SP-C promoter, Cre expression is targeted to the AECs in alveoli and peripheral bronchioles (Perl et al., 2009). *Flcn*$^{f/f}$*:SP-C-Cre* mice do not exhibit perinatal lethality or reduced survival, and weights were comparable across *Flcn*$^{f/f}$*:SP-C-Cre*, *Flcn*$^{wt/wt}$*:SP-C-Cre* and *Flcn*$^{f/wt}$*:SP-C-Cre* genotypes. The doxycycline diet did not affect mouse survival or weights and did not cause pulmonary distress. Genotyping, immunoblotting and co-immunostaining analyses of *Flcn*$^{f/f}$*:SP-C-Cre* mouse lungs confirmed *Flcn* deletion with doxycycline diet (Figures 1C, 1D, and 1E lower panels). Immunoblotting (Figure 1D, Dox+ lanes) shows residual Flcn expression in non SP-C-expressing cells in whole lung lysates. Importantly, inflation-fixed lungs from epithelial-specific *Flcn*-deleted mice exhibited alveolar enlargement (Figure 2A).

Morphometric lung measurements of mean linear intercept (MLI) and mean alveolar airspace area (MAAA) are significantly larger in lungs of epithelial-specific *Flcn*-deleted mice than in lung of *Flcn*-expressing *Flcn*$^{f/f}$*:SP-C-Cre* mice (Figures 2B, 2C, and Supplemental Figure S1D, S1E, and S1F). However, the overall structure and organization of the lungs are nearly normal. The lung alveoli of *Flcn*$^{wt/wt}$*:SP-C-Cre* or *Flcn*$^{f/wt}$*:SP-C-Cre* mice on regular or doxycycline-supplemental diet appear unchanged and comparable with lung of *Flcn*$^{f/f}$*:SP-C-Cre* mice on regular diet.

FLCN is required for postnatal lung alveolarization

To determine the role of FLCN during lung development, female *Flcn*$^{f/f}$*:SP-C-Cre* mice were placed on a doxycycline-supplemented diet starting at E0.5. Newborn pups were viable and appeared normal with no increased perinatal lethality. However, postnatal pups with lung epithelial-specific *Flcn* deletion exhibit larger alveoli compared to pups with *Flcn*-

expressing lung epithelium (Figures 2D, 2E and 2F). These data show developmental changes induced by FLCN deletion in lung epithelium and suggest a role for FLCN in branching morphogenesis of the lung.

FLCN regulates lung function

Morphological changes that resemble emphysema, such as alveolar enlargement, contribute to a decline in lung elastic recoil and pulmonary function. Lung function tests of adult *Flcn*$^{f/f}$*:SP-C-Cre* mice fed doxycycline for 6 weeks were markedly abnormal compared to age- and gender- matched littermates maintained on regular diet. Decreased airway elastance and resistance, and increased dynamic compliance were observed in *Flcn*$^{f/f}$*:SP-C-Cre* mice with *Flcn* deletion in lung epithelium compared to *Flcn*-expressing controls (Figure 2G).

To determine whether *Flcn* loss in other lung epithelial cells might also impair lung function, we generated *Flcn*$^{f/f}$*:CCSP-Cre* mice with targeted *Flcn* deletion in lung epithelial cells expressing Clara Cell Secretory Protein (CCSP) (Perl et al., 2009) (Figures S1G and S1H). CCSP-expressing lung epithelial cells localize in alveoli and bronchioles (Perl et al., 2009). *Flcn* deletion in *Flcn*$^{f/f}$*:CCSP-Cre* mice did not result in differences in the lung function (Figure S1I) compared to age- and gender-matched controls. These results demonstrate that lung parenchyma and function are affected by *Flcn* deletion specifically in AECs expressing SP-C, and alveolar epithelium is vulnerable to loss of FLCN during early lung development as well as in the mature lung.

FLCN is required for AEC survival *in vivo*

To evaluate whether apoptosis plays a role in airspace enlargement in BHD, control and BHD human lung tissues were immunostained with cleaved caspase-3 antibody. As seen in Figure 2H, apoptotic SP-C-positive cells were detected in BHD lung but not in control human lung. Alveolar epithelial cells positive for activated caspase-3 were identified in lungs of *Flcn*$^{f/f}$*:SP-C-Cre* mice maintained on a doxycycline diet compared to age- and gender-matched littermates maintained on regular diet (Figure 2I). TUNEL staining to assess DNA fragmentation was also detected in human BHD lungs and mouse lungs with deleted FLCN (Figure S2). Importantly, TUNEL staining co-localizes with SP-C immunostaining (Figure S2C).

FLCN downregulates LKB1 and controls AMPK activity

Since our results show that FLCN regulates AEC survival *in vivo*, we sought to identify the mechanism. AMPK activation is required to maintain epithelial cell-cell junctions, thus preserving epithelial barriers and promoting cell survival (Hardie, 2011). To determine whether FLCN deficiency affects AMPK activation, we used the *FLCN*-null human epithelial renal tumor cell line UOK257 derived from the kidney tumor of a BHD patient, and UOK257 cells with stably re-expressed FLCN (UOK257-2) used as a control (Baba et al., 2006).

AMPK is phosphorylated on Thr172 by LKB1 under conditions of stress, such as nutrient deprivation. Serum depletion of FLCN-expressing UOK257-2 cells for 24 and 48 hours resulted in time-dependent AMPK phosphorylation at Thr172 (Figure 3A). Phosphorylation

of acetyl-CoA-carboxylase (ACC) by activated AMPK also increased in a time-dependent manner in FLCN-expressing UOK257-2 cells. In contrast, *FLCN*-null cells exhibited reduced AMPK activation and ACC phosphorylation compared to *FLCN*-expressing UOK257-2 cells (Figure 3A). Importantly, serum deprivation also increased cleaved caspase-3 in *FLCN*-null UOK257 cells but not in *FLCN*-expressing UOK257-2 cells (Figure 3B).

To further examine the effect of FLCN loss on AMPK activation in lung epithelial cells, we isolated primary mouse AECs from lungs of $Flcn^{f/f}$*:SP-C-Cre* mice. Cells were treated with either an empty, replication-defective adenovirus or a replication-defective adenovirus expressing Cre-recombinase to delete *Flcn* (Figure 4A). Immunostaining with antibody against T1α, an alveolar epithelial cell marker (Ramirez et al., 2003), showed T1α expression in primary mouse AECs from $Flcn^{f/f}$*:SP-C-Cre* mice (Figure S3). AMPK(Thr172) phosphorylation was significantly decreased in *Flcn*-null AECs in contrast to *Flcn*-expressing AECs (Figure 4A). siRNA-induced Flcn knockdown in mouse epithelial NMuMG cells also significantly decreased AMPK(Thr172) phosphorylation compared to cells transfected with control siRNA (Figure 4B).

We next examined LKB1 levels in cells deficient for FLCN since LKB1 activates AMPK via phosphorylation at Thr172-AMPK (Hardie, 2011). LKB1 levels were reduced in primary AECs after *Flcn* deletion (Figure 4A). LKB1 levels were also markedly decreased in NMuMG cells with Flcn knockdown induced by siRNA (Figure 4B). To further determine whether LKB1 expression is regulated by FLCN, *FLCN*-null UOK257 cells were transduced with replication-defective adenovirus expressing FLCN. FLCN re-expression in *FLCN*-null UOK257 cells significantly increased LKB1 levels (Figure 4C). Cellular fractionation showed significantly increased LKB1 levels induced by FLCN expression not only in cytosol, but also in the membrane fraction (Figure 4C), confirming membrane localization of LKB1 (Sebbagh et al., 2009; Xu et al., 2013). These data suggest that FLCN regulates the cellular level and localization of LKB1.

Regulation of E-cadherin by FLCN

Evidence demonstrates that E-cadherin regulates membrane localization of LKB1, which is critical for AMPK activation (Sebbagh et al., 2009). Therefore, we determined whether *Flcn* deletion in primary AECs would affect E-cadherin expression and/or localization. E-cadherin is significantly decreased in the absence of Flcn expression (Figures 5A, 5B and 5C). Immunostaining also showed marked reduction of E-cadherin in the adherens junctions of cellular membranes (Figure 5D, upper panel, Figure S4A and Figure S4C). ZO-1 staining at tight junctions, however, appeared unchanged by *Flcn* deletion (Figure 5D, lower panel, Figure S4B, and Figure S4C). Thus, FLCN has a specific effect on E-cadherin expression and localization to adherens junctions.

To further determine FLCN's role in regulating E-cadherin, we used *TSC2*-null kidney epithelial cells, which have decreased membrane localization of E-cadherin (Figure 5E) (Barnes et al., 2010; Kleymenova et al., 2001). Transient transfection of *TSC2*-null cells with myc-tagged *FLCN* (Figure 5F) increased E-cadherin membrane localization, which was

statistically significant (Figure 5G). These data further suggest that FLCN may play a role in regulation of E-cadherin.

Increased *FLCN*-null epithelial cell permeability and apoptosis

Epithelial cell barriers and permeability depend on the preservation of adherens and tight junctions (Frisch and Screaton, 2001). Our data shows reduced E-cadherin localization in the *FLCN*-null cellular membrane, which might affect adherens junctions. Hence, we examined whether FLCN is required for maintenance of cell permeability. Primary AECs isolated from lungs of $Flcn^{f/f}$ mice were treated with empty adenovirus or Cre-recombinase-expressing adenovirus followed by a cell permeability assay using BODIPY-conjugated ouabain (DiPaolo and Margulies, 2012). Loss of *Flcn* resulted in increased permeability of primary AECs (Figure 5H) compared to cells expressing Flcn. In addition, loss of *Flcn* was associated with elevated cleaved caspase-3 levels and increased number of cells with DNA fragmentation detected by TUNEL assay (Figure 5I, 5J and 5K). These data demonstrate that FLCN is required for maintenance of epithelial barrier integrity and AEC survival.

Similarly, mouse epithelial NMuMG cells transfected with siRNA *Flcn* exhibited decreased membrane localization of E-cadherin (Figure 6A and Figure S5A). si*Flcn* also significantly decreased protein levels (Figure S5B) and *cdh1* (E-cadherin) and *stk11* (LKB1) gene expression (Figure S5D and S5F). Furthermore, in cells transfected with si*Flcn* E-cadherin does not maintain its multimeric structure as demonstrated by the presence of lower molecular weight staining under native conditions (Figure S5C), in contrast to no differences in LKB1 multimeric structure (Figure S5E) detected by native gel electrophoresis with equal loading of E-cadherin or LKB1 proteins.

Loss of *Flcn* in NMuMG cells also reduced trans-epithelial resistance (TER) (Figure 6B), another measure of increased cell permeability (Zheng and Cantley, 2007). We could not use TER to measure permeability of primary AECs because they grow on the Matrigel-coated plates which impede TER measurements. Finally, Flcn knockdown in NMuMG cells also increased cleaved caspase-3 levels (Figure 6C) and apoptosis (Figure 6D). Analysis of apoptotic gene expression using RT^2 Profiler PCR Arrays (SABiosciences, QIAGEN) revealed pro-apoptotic gene upregulation and decreased expression of pro-survival genes by Flcn knockdown (Figure S6A–S6C). Flcn-dependent downregulation of pro-survival *Bcl-2* gene was further confirmed by decreased levels of Bcl-2 protein levels (Figure S6D).

Collectively, our data show that FLCN regulates membrane localization of E-cadherin, protein and gene expression, maintains epithelial barrier function, and preserves epithelial cell survival.

AICAR and constitutively active AMPK rescue FLCN-deficient cell survival

Flcn knockdown visibly changes epithelial cell morphology with disruption of the cell monolayer (Figure 6E). To evaluate the role of AMPK in FLCN-deficient cell survival, mouse epithelial NMuMG cells were transfected with si*Flcn* and then treated with 5-aminoimidizole-4-carboxamide riboside (AICAR), a cell-permeable precursor of AMP that activates AMPK (Figure 6G). Treatment with AICAR reversed Flcn-induced disruption of

epithelial cell morphology (Figure 6E). AICAR treatment also significantly reduced Flcn-induced DNA fragmentation (Figure 6H) and epithelial cell death (Figure 6I). Similar results were seen upon transduction with adenovirus expressing the constitutively active AMPK (AdAMPK-CA) (Figure 6F) of NMuMG cells after Flcn knockdown. Expression of constitutively active AMPK markedly improved Flcn-deficient cell morphology (Figure 6E), reduced DNA fragmentation (Figure 6H), and rescued epithelial cell survival (Figure 6I). These results demonstrate that the kinase activity of AMPK is required for cell survival in the absence of FLCN.

AICAR improves alveolar surface tension in *Flcn$^{f/f}$:SP-C-Cre* mice

Our *in vitro* and *in vivo* data show that FLCN controls alveolar epithelial cell survival. Alveolar type 2 cells are the only cells capable of manufacturing and secreting phospholipids into alveoli to reduce surface tension and support alveolar inflation at low lung volumes. We therefore measured surface tension and phospholipid composition obtained from bronchoalveolar lavage (BAL) of *Flcn$^{f/f}$:SP-C-Cre* mice on regular or doxycycline-supplemented diet. Total phospholipids measured in large aggregate (LA) fractions of BAL from mice with *Flcn* deletion in lung epithelium were reduced compared to control mice (Figure 7A). In addition, we measured surface tension of LA phospholipids by a capillary surfactometer (Guttentag et al., 2005). The capillary surfactometer measures the ability of airflow to progress through a fluid filled capillary. The capillary openness, as a percentage of capillary diameter, is inversely related to the surface tension of the fluid in the capillary. LA phospholipids from doxycycline-treated *Flcn$^{f/f}$:SP-C-Cre* mice exhibited increased surface tension compared to untreated littermates, as evidenced by reduced capillary openness (Figure 7B). Importantly, AICAR treatment improved phospholipid content and the surface tension of LA from doxycycline-treated *Flcn$^{f/f}$:SP-C-Cre* mice (Figure 7A and 7B). There was a trend towards improved AEC survival, morphology, MLI and MAAA in doxycycline-treated *Flcn$^{f/f}$:SP-C-Cre* mice maintained on doxycycline and treated with AICAR compared to control mice also treated with AICAR (Figure 7C, E, F and G, respectively). Thus, Flcn deletion in lung epithelium induces a physiologically significant aberration in surface tension of alveolar phospholipids that is stabilized by AICAR treatment.

AICAR suppresses inflammation and MMP levels

Increased inflammation and proteolytic degradation of extracellular matrix components such as basement membrane or interstitial stroma are pathological changes characteristic of emphysema. To test whether loss of Flcn was associated with increased inflammation, we examined the BAL fluid for inflammatory cell influx. After 2 weeks on a doxycycline diet, *Flcn$^{f/f}$:SP-C-Cre* mice had increased numbers of total BAL cells compared with mice on regular diet that was further increased by 6 weeks on doxycycline (Figures S6 and 7D). Importantly, doxycycline-treated *Flcn$^{f/f}$:SP-C-Cre* mice treated with AICAR exhibited decreased inflammatory cell influx (Figure 7D).

We examined the pro-inflammatory cytokine profile of BAL from doxycycline-treated *Flcn$^{f/f}$:SP-C-Cre* mice and untreated littermates to determine whether loss of FLCN alters cytokine expression. We found marked elevations in interleukin-6 (IL-6) and macrophage

chemotactic protein-1 (MCP-1) in *Flcn*$^{f/f}$*:SP-C-Cre* mice on doxycycline compared to untreated littermates (Figure 7H and 7I). There were no significant differences between control mice and mice with *Flcn* deletion in AECs in the levels of eotaxin, GM-CSF, IFNγ, TNFα, IL-10, IL-13, IL-1β, KC, TGF-β1, VEGF and MIP1α (data not shown). Moreover, AICAR treatment lowered levels of IL-6 and MCP-1 in BAL fluid of mice with *Flcn* knock-out.

MMPs represent a family of structurally and functionally related enzymes responsible for the proteolytic degradation of extracellular matrix and have been mechanistically linked with progressive pulmonary emphysema and chronic inflammation. BAL from doxycycline-treated *Flcn*$^{f/f}$*:SP-C-Cre* mice demonstrated significant elevations of MMP-3 and MMP-9 compared to untreated mice (Figure 7J and 7K). Furthermore, treatment with AICAR lowered MMP-3 and MMP-9 levels to levels comparable to control mice (Figure 7J and 7K). Collectively, *in vivo* experiments demonstrate that Flcn inactivation in lung AECs of *Flcn*$^{f/f}$*:SP-C-Cre* mice evokes inflammatory response and upregulation of MMP-3 and MMP-9 in a manner that is reversible with exogenous AMPK activation by AICAR.

Discussion

The present study identifies FLCN as a novel regulator of lung homeostasis and advances our understanding of the pathophysiology of emphysema. This study details the cellular and molecular mechanisms by which FLCN contributes to lung epithelial cell survival, thereby maintaining alveolar surface tension through maintenance of phospholipid production. As such, loss of FLCN leads to loss of epithelial cells with resultant reduction in phospholipid production that contributes to the lung changes associated with BHD (Figure 7I). Furthermore, we show that FLCN maintains epithelial cell junctions and survival in an AMPK-dependent fashion by regulating membrane localization of E-cadherin and LKB1 (Figure 7I).

The abnormal enlargement of airspaces is a major pathological manifestation of many common and rare lung diseases including emphysema, cystic fibrosis, chronic obstructive pulmonary disease (COPD), pulmonary lymphangioleiomyomatosis (LAM), pulmonary Langerhans cell histocytosis (PLCH), lymphocytic interstitial pneumonia (LIP), follicular bronchiolitis, light chain deposition disease, Sjogren's syndrome and amyloidosis (Gupta et al., 2013). It is becoming increasingly clear that the mechanisms underlying the development of emphysematous changes in the lung are more complex than simply an imbalance of proteolysis/antiproteolysis. Together, our data provide additional supportive evidence for the complex pathophysiology of emphysematous alveolar enlargement by showing that FLCN supports cell survival and influences the cytokine and matrix metalloproteinase milieu in ways that might contribute to lung cyst formation with loss of FLCN in BHD. These novel insights into the role of FLCN may serve as a foundation for novel therapeutic approaches for BHD and other emphysematous lung diseases.

This study establishes that FLCN plays an important physiological role in regulating alveolar epithelial cell survival and alveolar integrity. We demonstrate the importance of FLCN for alveolar epithelial cell apoptosis *in vivo* and *in vitro* using *Flcn*$^{f/f}$*:SP-C-Cre* mice,

by examining both lung tissue and isolated AECs. It is intriguing that Flcn loss in an immortalized mouse embryonic stem cell line resulted in transcriptional down-regulation of pro-apoptotic protein Bim (Cash et al., 2011). Elucidating a more direct role for Flcn intersecting with apoptotic pathways will be possible in the future with our cell and mouse models.

Our studies clearly demonstrate that the pro-survival role is mediated through AMPK (Figure 7I). The pro-survival role of AMPK in epithelial cells is well established, especially as related to energy status of cells, and extends to the maintenance of epithelial contacts and polarity (Mirouse et al., 2007; Zhang et al., 2006; Zheng and Cantley, 2007). Phosphorylation of AMPK by tumor suppressor LKB1 increases AMPK activity (Jansen et al., 2009), providing a means of coordinating epithelial cell polarity and proliferation with cellular energy status (Mirouse et al., 2007). This requires the localization of LKB1 to E-cadherin at adherens junctions (Sebbagh et al., 2009). Evidence suggesting a role for AMPK in microtubule formation via CLIP-170 (Nakano et al., 2010), which also has a role in E-cadherin localization (Barnes, 2010) provides a reinforcing loop of E-cadherin/LKB1/AMPK regulation of apical polarity.

Our data suggest that FLCN promotes survival of alveolar epithelial cells through this E-cadherin/LKB1/AMPK axis. Our data also suggest that FLCN functions upstream of AMPK. Loss of FLCN affects assembly of adherens junctions via downregulation of E-cadherin levels while having little effect on ZO1 levels in tight junctions. Importantly, disruption of the epithelial monolayer and apoptosis caused by FLCN loss was prevented by either molecular or pharmacological AMPK activation. Together with published studies, our data suggest that FLCN is required for E-cadherin dependent epithelial cell-cell junctions, impairment of LKB1-AMPK signaling and caspase-dependent apoptosis of lung AECs, the initial component of alveolar airspace enlargement. Further studies will provide detail mechanism how FLCN regulate E-cadherin and LKB1 expressions.

One consequence of altered alveolar epithelial cell survival is the loss of an important source of pulmonary phospholipids. Phospholipids play an important role in the maintenance of alveolar stability through the respiratory cycle, so it is perhaps not surprising that apoptosis-induced airspace enlargement is associated with increased alveolar surface tension, and alveolar instability and collapse (Mouded et al., 2009). However, this raises an important therapeutic possibility, specifically the potential for exogenous phospholipid therapy to mitigate the effects of alveolar epithelial cell loss. Though exogenous phospholipid therapy for unintubated patients is currently unfeasible due to issues of delivery, novel delivery modalities or therapies targeting increased production of phospholipid by the remaining epithelial cell population are attractive options for the future.

The loss of FLCN also evokes an inflammatory response associated with local production of inflammatory cytokines and MMPs. Further studies will determine whether this is due to an epithelial injury response, or whether FLCN itself signals an anti-inflammatory pathway.

FLCN acts through an AMPK-mediated pathway that can be resurrected by exogenous activation of AMPK. AICAR, an AMPK activator, reverses many of the pathologic changes

in the *Flcn*$^{f/f}$*:SP-C-Cre* mice with *Flcn* deletion limited to lung AECs. Importantly, AICAR rescues those features of Flcn loss that are critical to the pathophysiology of lung cysts, specifically mitigating inflammation and matrix metalloproteinase expression that propagate local alveolar damage, and enhancing phospholipid production to stabilize airspace inflation. While AMPK-dependent suppression of MMP-9 has been previously reported (Hwang and Jeong, 2010; Morizane et al., 2011), our data provide an attractive mechanism for a feed-forward cycle of epithelial cell destabilization with loss of FLCN followed by further local destruction by enhanced MMP production. Further studies are needed to establish the mechanism(s) whereby impaired AMPK signaling increases MMP expression.

Rescue by AICAR does not reverse the structural changes due to FLCN loss. It does not rule out the possibility that AMPK agonists may have a role in prevention or that they may be useful to stop or slow the progression of existing emphysema.

There are several limitations of our studies. First, *Flcn* deletion in *Flcn*$^{f/f}$*:SP-C-Cre* mice does not precisely phenocopy lung changes in patients with BHD. Patients with BHD exhibit loss of alveoli and lung cyst development predominantly localized to the lower regions of the lung (Gupta et al., 2013). The differences between our mouse model and human patients may be due to either the restricted knockout of *Flcn* in epithelial cells only, or may be due to expression of non-null mutations of FLCN in BHD patients. Despite these limitations, our data demonstrate the key role of FLCN in maintenance of normal lung parenchyma architecture and physiology, and a well-defined mechanism whereby FLCN, acting through E-cadherin, LKB1 and AMPK, has a critical role in regulating the assembly of epithelial cell junctions.

Experimental Procedures

The human lung tissue

Control human lung tissues from three subjects were obtained from the National Disease Research Interchange, and the human BHD tissue samples from four BHD patients were obtained from the NIH under approved protocols.

Animals

Flcn$^{f/f}$*:SP-C-Cre* mice were generated by crossing *Flcn*$^{f/f}$ mice (Baba et al., 2008) with *SP-C-rtTA/tetO-Cre* (line 2) mice (Perl et al., 2009). *Flcn*$^{f/f}$*:CCSP-C-Cre* mice were generated by crossing *Flcn*$^{f/f}$ mice with *CCSP-rtTA/tetO-Cre* mice (line 2) (Perl et al., 2009). Genotyping was performed as described (Baba et al., 2008). Six-week-old male *Flcn*$^{f/f}$*:SP-C-Cre* or *Flcn*$^{f/f}$*:CCSP-C-Cre* mice were transferred on chow supplemented with 2.5% doxycycline (Dox+) or maintained on regular chow (Dox−) for 3 or 6 weeks. Treatment with 500 mg/kg AICAR was performed daily by intraperitoneal injections for 6 weeks in mice on Dox− or Dox+ diet.

Lung function was measured on computerized FlexiVent System (Scireq, Montreal, Canada) (Haczku et al., 2002). For morphological analyses, lungs were inflated at constant 25-cm H_2O pressure with 1:1 OCT/PBS or low melting agarose in PBS for approximately 8 min (Goncharova et al., 2012). Each experimental group included a minimum of five animals per

condition. Experiments to determine effects of Flcn loss on alveoli space enlargement were performed three times, and experiments with treatment by AICAR were performed twice. All animal procedures were performed according to a protocol approved by the University of Pennsylvania IACUC.

BAL analyses

BAL fluid was collected by lavaging the lung with 1 ml of sterile saline to a total of 5 ml. Recovered BAL was centrifuged 400×g for 10 min at 4°C, then cell pellet was resuspended in 1 ml PBS for total cell count. Cell-free BAL supernatants were separated by centrifugation at 20,000×g for 60 min at 4°C into large-aggregate (LA) and small-aggregate (SA) phospholipid fractions. Surface tension was determined by measuring capillary openness with a capillary a surfactometer (Calmia Medical, Inc., Toronto, Canada) (Guttentag et al., 2005). Briefly, 0.5 μL of 1 mg/ml LA fraction was deposited into the glass capillary and compressed for 120 seconds, resulting in cyclic extrusion from narrow end of capillary permitting airflow and capillary patency. Dysfunctional phospholipids exhibit decreased capillary patency which is inversely correlated with the surface tension. Microprocessor calculates the percentage of the 120-s period that the capillary is open to free airflow. Each sample was analyzed in triplicate.

Cytokine and MMPs were determined in the cell-free BAL by Searchlight multiplex ELISA at Aushon Biosystems (Aushon, Billerica, MA).

Morphometry

Images of lung tissue sections stained with H&E were acquired with a Nikon Eclipse 80i microscope under 100x magnification. Ten randomly selected fields per slide from three nonserial sections were analyzed. Image-Pro Plus 6.2 software (Media Cybernetics Inc.) was used to measure the MAAA and MLI. Airway, vascular structures, and histological mechanical artifacts were eliminated from the analysis.

Immunohistochemical, immunocytochemical and immunoblot analyses were performed as described (Goncharova et al., 2011). Immunostaining was visualized with Leica SP5 X, Zeiss LSM 700 confocal microscope, or Nikon Eclipse TE2000-E microscope equipped with an Evolution QEi digital video camera under appropriate filters. Protein levels were analyzed by optical density with Gel-Pro Analyzer software.

Cell culture

AECs were isolated from 2-week-old *Flcn*$^{f/f}$ mice as described (Atochina-Vasserman et al., 2011). Mouse lungs were inflated *in situ* via tracheal cannulation with Dispase. Dissected lobes were digested in MEM + DNase I. The mixed cells were filtered, and fibroblasts were removed from the suspension by 3 successive adherence steps on plastic. Negative selection was used to purify epithelial cells from macrophages and other blood cells using magnetic beads (Dynal Mouse T Cell Negative Isolation Kit #114.13D). Cells were plated in HITES medium (prepared in Ham's F12 + 15 mM HEPES, 0.8 mM CaCl2, hydrocortisone, β-estradiol) + 10% FCS on coverslips coated with 10% Matrigel (BD Biosciences) for immunofluorescence staining. Serum was added for 48h to facilitate adherence and was then

removed to minimize overgrowth of any remaining fibroblasts. Human UOK-257 and UOK257-2 cell lines (Hong et al., 2010), and TSC2-null kidney epithelial cells from Eker rat were described (Kleymenova et al., 2001); mouse epithelial NMuMG cells were purchased from the American Type Culture Collection.

Flcn siRNA was from Dharmacon RNA Technologies (Lafayette, CO) and scrambled siRNA was from Santa Cruz Biotechnologies (Santa Cruz, CA). Transfection was performed using Effectene or RNAiFect reagents (QIAGEN), respectively. Infection with AdCre or AdFLCN adenovirus was described (Goncharova et al., 2004).

BODIPY permeability assay

The assay was performed as described (DiPaolo and Margulies, 2012). Briefly, 2μm BODIPY-ouabain (Invitrogen) was added to AECs for 1 h. Then BODIPY-ouabain fluorescence was visualized using a green emission filter. Fluorescence was measured on 4 separate fields per well, and 3 wells were measured per condition. All measurements were normalized to values from cells infected with control adenovirus.

Trans-epithelial resistance was measured in confluent NMuMG cells, grown on electric cell-substrate impedance sensing (ECIS) 8W1E plates, then subjected to an elevated voltage pulse of 40 kHz frequency, 3.5 V amplitude for 30 s (Taliaferro-Smith et al., 2009).

Data analysis

Data points from individual assays represent mean ± SE. Statistically significant differences among groups were assessed with ANOVA (with the Fisher PLSD post-hoc test), with values of $p < 0.05$ sufficient to reject the null hypothesis for all analyses. In Figures 7 and S7, statistically significant differences among groups were assessed with t-test, n = 5–7 animals per group. All experiments were designed with matched control conditions within each experiment (minimum of five animals) to enable statistical comparison as paired samples and to obtain statistically significant data.

Supplementary Material

Refer to Web version on PubMed Central for supplementary material.

Acknowledgments

We thank Dr. Jeffrey A. Whitsett, Cincinnati Children's Hospital Medical Center, for generously providing *SP-C-rtTA/tetO-Cre* (line 2) mice and *CCSP-rtTA/tetO-Cre* (line 2); Dr. Cheryl Walker, Texas A&M Health Science Center, for generous gift of rat TSC2-null cells; Dr. Leslie A. Litzky, University of Pennsylvania, for help with BHD patients' tissue specimens; Dr. Chang-Jiang Guo and Helen Abramova, Rutgers University, for excellent technical support; Ms. Sharmin Islam for preparing Figure S1A, and Mr. Nathan Tessema Ersumo for exceptional help with Figures 1 and 2, graphical abstract, slider image, and technical assistance with the manuscript. This research was supported by the Intramural Research Program of NIH, Frederick National Laboratory for Cancer Research, Center for Cancer Research. This project has been funded in whole or in part with federal funds from the Frederick National Laboratory for Cancer Research, NIH, under contract HHSN261200800001E. The content of this publication does not necessarily reflect the views or policies of the DHHS, nor does mention of trade names, commercial products or organizations imply endorsement by the US Government. This work was supported by NIH/NHLBI RO1 HL110551 (V.P.K.) and the Myrovlytis Trust (S.B.H. and V.P.K.).

References

Atochina-Vasserman EN, Bates SR, Zhang P, Abramova H, Zhang Z, Gonzales L, Tao J-Q, Gochuico BR, Gahl W, Guo C-J, et al. Early Alveolar Epithelial Dysfunction Promotes Lung Inflammation in a Mouse Model of Hermansky Pudlak Syndrome. Am J Respir Crit Care Med. 2011:201011–201882OC.

Baba M, Furihata M, Hong SB, Tessarollo L, Haines DC, Southon E, Patel V, Igarashi P, Alvord WG, Leighty R, et al. Kidney-Targeted Birt-Hogg-Dube Gene Inactivation in a Mouse Model: Erk1/2 and Akt-mTOR Activation, Cell Hyperproliferation, and Polycystic Kidneys. J Natl Cancer Inst. 2008; 100:140–154. [PubMed: 18182616]

Baba M, Hong S-B, Sharma N, Warren MB, Nickerson ML, Iwamatsu A, Esposito D, Gillette WK, Hopkins RF III, Hartley JL, et al. Folliculin encoded by the BHD gene interacts with a binding protein, FNIP1, and AMPK, and is involved in AMPK and mTOR signaling. Proc Natl Acad Sci USA. 2006; 103:15552–15557. [PubMed: 17028174]

Barnes EA, Kenerson HL, Jiang X, Yeung RS. Tuberin Regulates E-Cadherin Localization: Implications in Epithelial-Mesenchymal Transition. Am J Pathol. 2010; 177:1765–1778. [PubMed: 20813961]

Barnes PJ. Neutrophils Find Smoke Attractive. Science. 2010; 330:40–41. [PubMed: 20929796]

Birt AR, Hogg GR, Dube WJ. Hereditary multiple fibrofolliculomas with trichodiscomas and acrochordons. Arch Derm. 1977; 113:1674–1677. [PubMed: 596896]

Cash TP, Gruber JJ, Hartman TR, Henske EP, Simon MC. Loss of the Birt-Hogg-Dube tumor suppressor results in apoptotic resistance due to aberrant TGFb-mediated transcription. Oncogene. 2011; 30:2534–2546. [PubMed: 21258407]

DiPaolo BC, Margulies SS. Rho kinase signaling pathways during stretch in primary alveolar epithelia. Am J Physiol Lung Cell Mol Physiol. 2012; 302:L992–L1002. [PubMed: 22287611]

Frisch SM, Screaton RA. Anoikis mechanisms. Curr Opin Cell Biol. 2001; 13:555–562. [PubMed: 11544023]

Goncharova E, Goncharov D, Noonan D, Krymskaya VP. TSC2 modulates actin cytoskeleton and focal adhesion through TSC1-binding domain and the Rac1 GTPase. J Cell Biol. 2004; 167:1171–1182. [PubMed: 15611338]

Goncharova EA, Goncharov DA, Fehrenbach M, Khavin I, Duka B, Hino O, Colby TV, Merrilees MJ, Haczku A, Albelda SM, et al. Prevention of Alveolar Destruction and Airspace Enlargement in a Mouse Model of Pulmonary Lymphangioleiomyomatosis (LAM). Sci Transl Med. 2012; 4:154ra134.

Goncharova EA, Goncharov DA, Li H, Pimtong W, Lu S, Khavin I, Krymskaya VP. mTORC2 Is Required for Proliferation and Survival of TSC2-Null Cells. Mol Cell Biol. 2011; 31:2484–2498. [PubMed: 21482669]

Gupta N, Seyama K, McCormack F. Pulmonary manifestations of Birt-Hogg-Dubé syndrome. Fam Cancer. 2013:1–10. [PubMed: 23377869]

Guttentag SH, Akhtar A, Tao JQ, Atochina E, Rusiniak ME, Swank RT, Bates SR. Defective Surfactant Secretion in a Mouse Model of Hermansky-Pudlak Syndrome. Am J Respir Cell Mol Biol. 2005; 33:14–21. [PubMed: 15790974]

Haczku A, Atochina EN, Tomer Y, Cao Y, Campbell C, Scanlon ST, Russo SJ, Enhorning G, Beers MF. The late asthmatic response is linked with increased surface tension and reduced surfactant protein B in mice. Am J Physiol Lung Cell Mol Physiol. 2002; 283:L755–L765. [PubMed: 12225952]

Hardie DG. AMP-activated protein kinase—an energy sensor that regulates all aspects of cell function. Gene Develop. 2011; 25:1895–1908. [PubMed: 21937710]

Hasumi H, Baba M, Hasumi Y, Huang Y, Oh H, Hughes RM, Klein ME, Takikita S, Nagashima K, Schmidt LS, et al. Regulation of Mitochondrial Oxidative Metabolism by Tumor Suppressor FLCN. J Natl Cancer Inst. 2012; 104:1750–1764. [PubMed: 23150719]

Hasumi H, Baba M, Hong SB, Hasumi Y, Huang Y, Yao M, Valera VA, Linehan WM, Schmidt LS. Identification and characterization of a novel folliculin-interacting protein FNIP2. Gene. 2008; 415:60–67. [PubMed: 18403135]

Hasumi Y, Baba M, Ajima R, Hasumi H, Valera VA, Klein ME, Haines DC, Merino MJ, Hong SB, Yamaguchi TP, et al. Homozygous loss of BHD causes early embryonic lethality and kidney tumor development with activation of mTORC1 and mTORC2. Proc Natl Acad Sci. 2009; 106:18722–18727. [PubMed: 19850877]

Henson PM, Tuder RM. Apoptosis in the lung: induction, clearance and detection. Am J Physiol Lung Cell Mol Physiol. 2008; 294:L601–611. [PubMed: 18178675]

Hong SB, Oh H, Valera V, Stull J, Ngo DT, Baba M, Merino M, Linehan WM, Schmidt L. Tumor suppressor FLCN inhibits tumorigenesis of a FLCN-null renal cancer cell line and regulates expression of key molecules in TGF-beta signaling. Mol Canc. 2010; 9:160.

Hwang YP, Jeong HG. Metformin blocks migration and invasion of tumour cells by inhibition of matrix metalloproteinase-9 activation through a calcium and protein kinase Cα-dependent pathway: phorbol-12-myristate-13-acetate-induced/extracellular signal-regulated kinase/activator protein-1. Br J Pharmacol. 2010; 160:1195–1211. [PubMed: 20590612]

Jansen M, ten Klooster JP, Offerhaus GJ, Clevers H. LKB1 and AMPK Family Signaling: The Intimate Link Between Cell Polarity and Energy Metabolism. Physiol Rev. 2009; 89:777–798. [PubMed: 19584313]

Kleymenova E, Ibragimov-Beskrovnaya O, Kugoh H, Everitt J, Xu H, Kiguchi K, Landes G, Harris P, Walker C. Tuberin-dependent membrane localization of polycystin-1: a functional link between polycystic kidney disease and the *TSC2* tumor suppressor gene. Mol Cell. 2001; 7:823–832. [PubMed: 11336705]

Lee YM, Lee JO, Jung JH, Kim JH, Park SH, Park JM, Kim EK, Suh PG, Kim HS. Retinoic Acid Leads to Cytoskeletal Rearrangement through AMPK-Rac1 and Stimulates Glucose Uptake through AMPK-p38 MAPK in Skeletal Muscle Cells. J Biol Chem. 2008; 283:33969–33974. [PubMed: 18927084]

Liu C, Liang B, Wang Q, Wu J, Zou MH. Activation of AMP-activated Protein Kinase 1a Alleviates Endothelial Cell Apoptosis by Increasing the Expression of Anti-apoptotic Proteins Bcl-2 and Survivin. J Biol Chem. 2010; 285:15346–15355. [PubMed: 20233722]

Liu W, Chen Z, Ma Y, Wu X, Jin Y, Hou S. Genetic Characterization of the *Drosophila* Birt-Hogg-Dubé Syndrome Gene. PLoS ONE. 2013; 8:e65869. [PubMed: 23799055]

Makowski L, Hayes DN. Role of LKB1 in lung cancer development. Br J Cancer. 2008; 99:683–688. [PubMed: 18728656]

Mirouse V, Swick LL, Kazgan N, St Johnston D, Brenman JE. LKB1 and AMPK maintain epithelial cell polarity under energetic stress. J Cell Biol. 2007; 177:387–392. [PubMed: 17470638]

Morizane Y, Thanos A, Takeuchi K, Murakami Y, Kayama M, Trichonas G, Miller J, Foretz M, Viollet B, Vavvas DG. AMP-activated Protein Kinase Suppresses Matrix Metalloproteinase-9 Expression in Mouse Embryonic Fibroblasts. J Biol Chem. 2011; 286:16030–16038. [PubMed: 21402702]

Mouded M, Egea EE, Brown MJ, Hanlon SM, Houghton AM, Tsai LW, Ingenito EP, Shapiro SD. Epithelial Cell Apoptosis Causes Acute Lung Injury Masquerading as Emphysema. Am J Respir Cell Mol Biol. 2009; 41:407–414. [PubMed: 19188661]

Nakano A, Kato H, Watanabe T, Min KD, Yamazaki S, Asano Y, Seguchi O, Higo S, Shintani Y, Asanuma H, et al. AMPK controls the speed of microtubule polymerization and directional cell migration through CLIP-170 phosphorylation. Nat Cell Biol. 2010; 12:583–590. [PubMed: 20495555]

Nickerson ML, Warren MB, Toro JR, Matrosova V, Glenn G, Turner ML, Duray P, Merino M, Choyke P, Pavlovich CP. Mutations in a novel gene lead to kidney tumors, lung wall defects, and benign tumors of the hair follicle in patients with the Birt-Hogg-Dube syndrome. Canc Cell. 2002; 2:157–164.

Perl AK, Zhang L, Whitsett JA. Conditional Expression of Genes in the Respiratory Epithelium in Transgenic Mice. Am J Respir Cell Mol Biol. 2009; 40:1–3. [PubMed: 19075182]

Ramirez MI, Millien G, Hinds A, Cao Y, Seldin DC, Williams MC. T1α, a lung type I cell differentiation gene, is required for normal lung cell proliferation and alveolus formation at birth. Dev Biol. 2003; 256:62–73.

Schmidt LS. Birt-Hogg-Dubé syndrome, a genodermatosis that increases risk for renal carcinoma. Curr Mol Med. 2004; 4:877–885. [PubMed: 15579035]

Schmidt LS, Warren MB, Nickerson ML, Weirich G, Matrosova V, Toro JR, Turner ML, Duray P, Merino M, Hewitt S, et al. Birt-Hogg-Dubé Syndrome, a Genodermatosis Associated with Spontaneous Pneumothorax and Kidney Neoplasia, Maps to Chromosome 17p11.2. Am J Hum Genet. 2001; 69:876–882. [PubMed: 11533913]

Sebbagh M, Santoni MJ, Hall B, Borg JP, Schwartz MA. Regulation of LKB1/STRAD Localization and Function by E-Cadherin. Curr Biol. 2009; 19:37–42. [PubMed: 19110428]

Shapiro SD, Ingenito EP. The Pathogenesis of Chronic Obstructive Pulmonary Disease. Am J Respir Cell Mol Biol. 2005; 32:367–372. [PubMed: 15837726]

Suki B, Lutchen KR, Ingenito EP. On the Progressive Nature of Emphysema: Roles of Proteases, Inflammation, and Mechanical Forces. Am J Respir Crit Care Med. 2003; 168:516–521. [PubMed: 12941655]

Takagi Y, Kobayashi T, Shiono M, Wang L, Piao X, Sun G, Zhang D, Abe M, Hagiwara Y, Takahashi K, et al. Interaction of folliculin (Birt-Hogg-Dube gene product) with a novel Fnip1-like (FnipL// Fnip2) protein. Oncogene. 2008; 27:5339–5347. [PubMed: 18663353]

Taliaferro-Smith L, Nagalingam A, Zhong D, Zhou W, Saxena NK, Sharma D. LKB1 is required for adiponectin-mediated modulation of AMPK-S6K axis and inhibition of migration and invasion of breast cancer cells. Oncogene. 2009; 28:2621–2633. [PubMed: 19483724]

van Slegtenhorst M, Khabibullin D, Hartman TR, Nicolas E, Kruger WD, Henske EP. The Birt-Hogg-Dube and Tuberous Sclerosis Complex Homologs Have Opposing Roles in Amino Acid Homeostasis in Schizosaccharomyces pombe. J Biol Chem. 2007; 282:24583–24590. [PubMed: 17556368]

Vocke CD, Yang Y, Pavlovich CP, Schmidt LS, Nickerson ML, Torres-Cabala CA, Merino MJ, Walther MM, Zbar B, Linehan WM. High Frequency of Somatic Frameshift BHD Gene Mutations in Birt-Hogg-Dubé–Associated Renal Tumors. J Natl Cancer Inst. 2005; 97:931–935. [PubMed: 15956655]

Xu X, Jin D, Durgan J, Hall A. LKB1 Controls Human Bronchial Epithelial Morphogenesis through p114RhoGEF-Dependent RhoA Activation. Mol Cell Biol. 2013; 33:2671–2682. [PubMed: 23648482]

Zhang L, Li J, Young LH, Caplan MJ. AMP-activated protein kinase regulates the assembly of epithelial tight junctions. Proc Natl Acad Sci. 2006; 103:17272–17277. [PubMed: 17088526]

Zheng B, Cantley LC. Regulation of epithelial tight junction assembly and disassembly by AMP-activated protein kinase. Proc Natl Acad Sci USA. 2007; 104:819–822. [PubMed: 17204563]

Highlights

- FLCN plays an essential role in epithelial cell integrity and lung homeostasis
- FLCN is required for lung alveolar epithelial cell survival
- FLCN modulates E-cadherin, LKB1 and AMPK activation
- FLCN loss is a key event in emphysematous lung changes in Birt-Hogg-Dubé syndrome

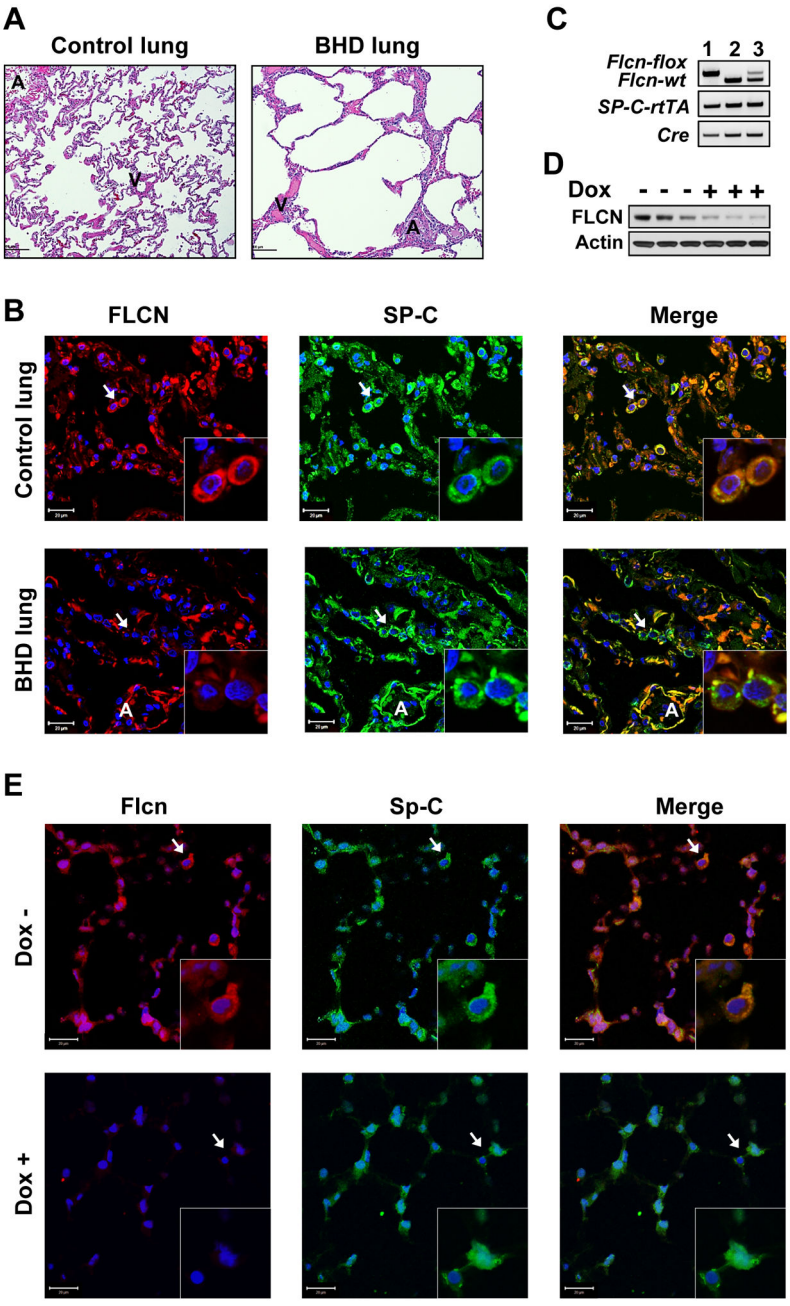

Figure 1. Lung histology and FLCN and SP-C immunostaining

(A) H&E staining of normal human lung (Control) (n=3) and BHD lung (n=4).

(B) FLCN-positive (red) AECs (SP-C, green) are seen in normal human lung (n=3) but not in BHD (n=4) lungs. DAPI (blue) stains nuclei.

(C) Genotyping of homozygous *Flcn*$^{f/f}$*:SP-C-Cre* (1), wild-type *Flcn*$^{wt/wt}$*:SP-C-Cre* (2), and heterozygous *Flcn*$^{wt/f}$*:SP-C-Cre* mice (3).

(D) Flcn levels in whole lung lysates from *Flcn*$^{f/f}$*:SP-C-Cre* mice on doxycycline (Dox+) for 6 weeks (n=3) or regular (Dox-) diet (n=3).

(E) Loss of Flcn (red) in lung AECs (SP-C, green) in *Flcn*$^{f/f}$*:SP-C-Cre* mice treated as in (D).

Scale bars, 20 μM.

A – conducting airways; V- blood vessels.

See also Figure S1.

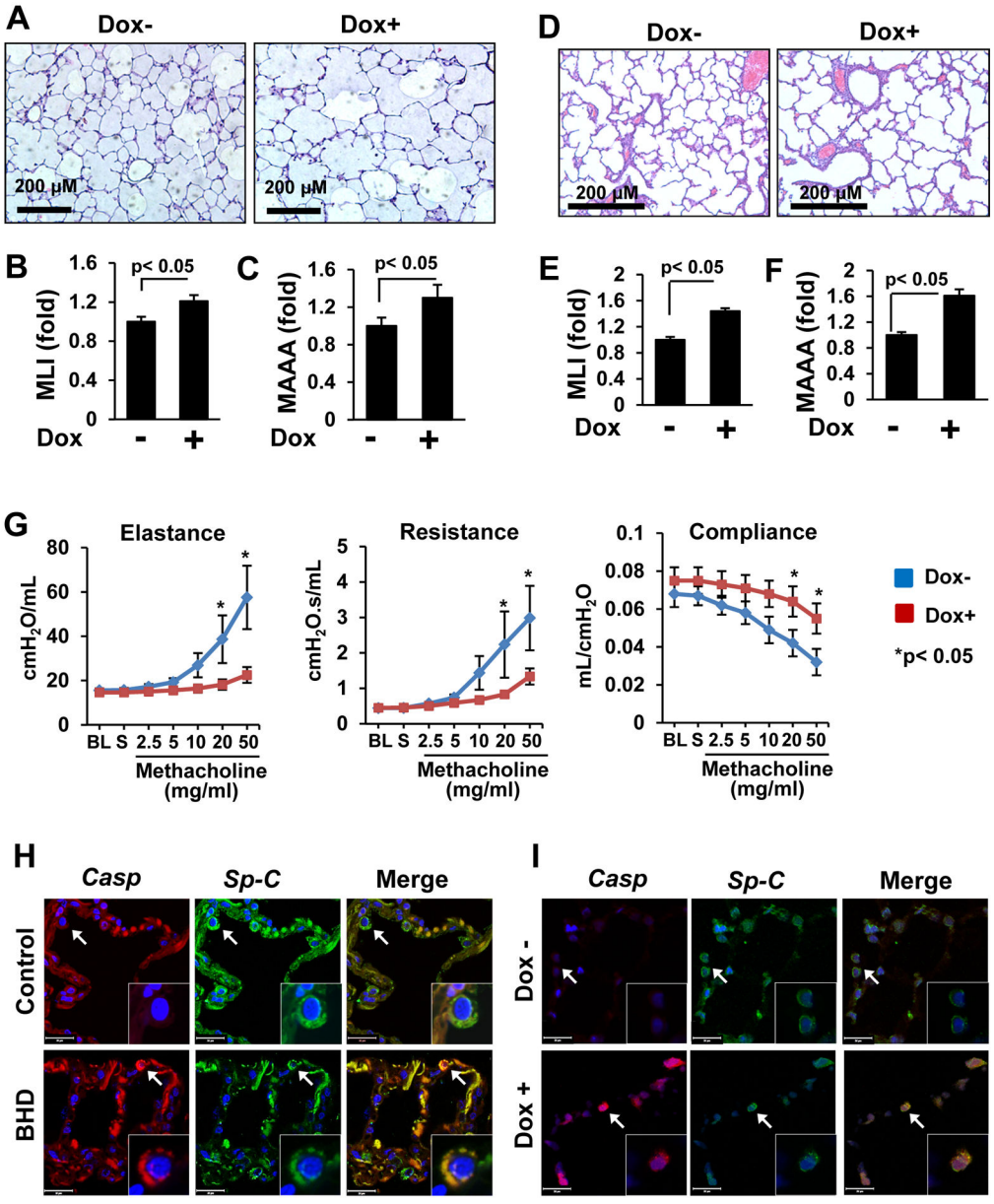

Figure 2. Loss of FLCN increases pulmonary alveoli, impairs lung function and induces alveolar epithelial cell apoptosis

(A–C) Flcn loss results in alveolar enlargement in *Flcn*$^{f/f}$*:SP-C-Cre* mice treated as in (1D). Scale bars, 200 μM.

(D–F) Enlarged alveoli in pups with FLCN deletion in lung epithelium. Scale bars, 200 μM.

(G) FLCN deletion in *Flcn*$^{f/f}$*:SP-C-Cre* mice impairs lung function, n=8 per group. BL–baseline; S-saline.

The mean is shown; error bars represent SE (n>3). Data for Dox- mice are taken as one fold.

(H) Cleaved caspase-3-positive (red) cells in lung epithelium (SP-C, green) of BHD lung, (n=5) but not in control (n=3) lung.

(I) Loss of Flcn in lung epithelium (SP-C, green) results in alveolar epithelial cell apoptosis (red) in lung from *Flcn*$^{f/f}$*:SP-C-Cre* mice treated as in (1D), n=3 per group.

Scale bars, 20 μM.

See also Figure S2.

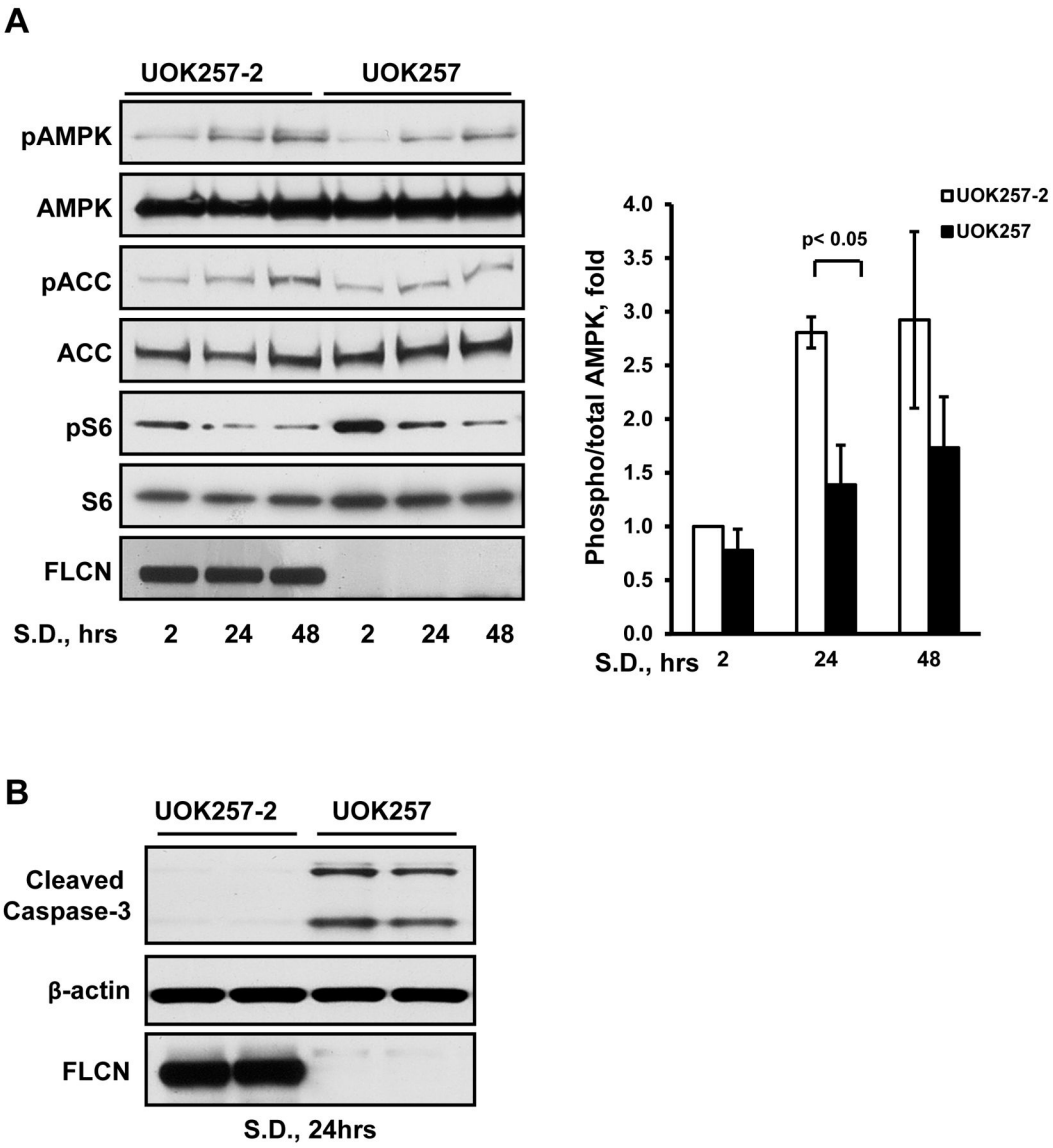

Figure 3. ***FLCN*** **loss impairs AMPK activation and upregulates cleaved caspase-3**

(A) *FLCN*-null UOK257 and FLCN-expressing UOK257-2 epithelial cells were serum deprived (S.D.) in DMEM supplemented with 0.1% BSA. Data are mean ± SE, n=3. **(B)** Energy depletion of FLCN-null UOK257 cells upregulates cleaved caspase-3.

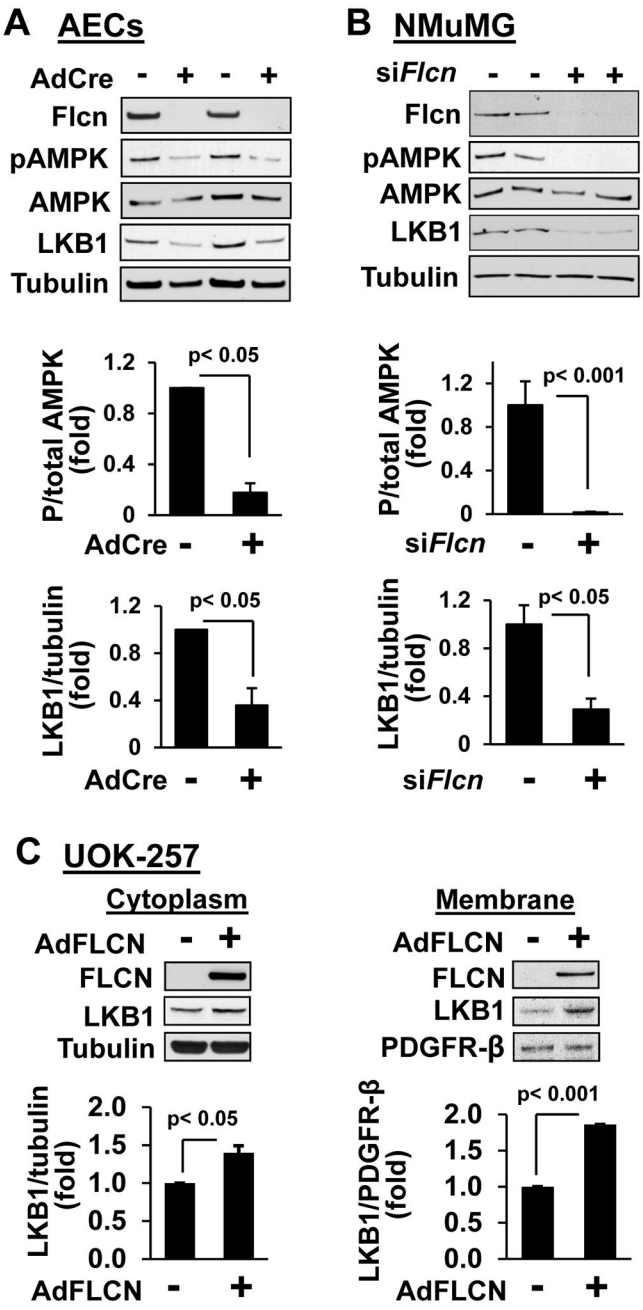

Figure 4. FLCN regulates LKB1 levels and AMPK phosphorylation

(A) Primary lung AECs from *FLCN*$^{f/f}$ mice were infected with control (−) or Cre-recombinase-expressing adenovirus (AdCre,+) followed by immunoblot analysis. See also Figure S3.

(B) Immunoblot analyses of mouse epithelial NMuMG cells transfected with *Flcn* siRNA (si*Flcn*) or control scrambled siRNA (−).

(C) Re-expression of FLCN in human *FLCN*-null UOK-257 cells increases membrane localization of LKB1.

Top: representative images. Bottom: statistical analyses. Protein ratio for control cells were taken as one fold. Data are mean ± SE, n=3.

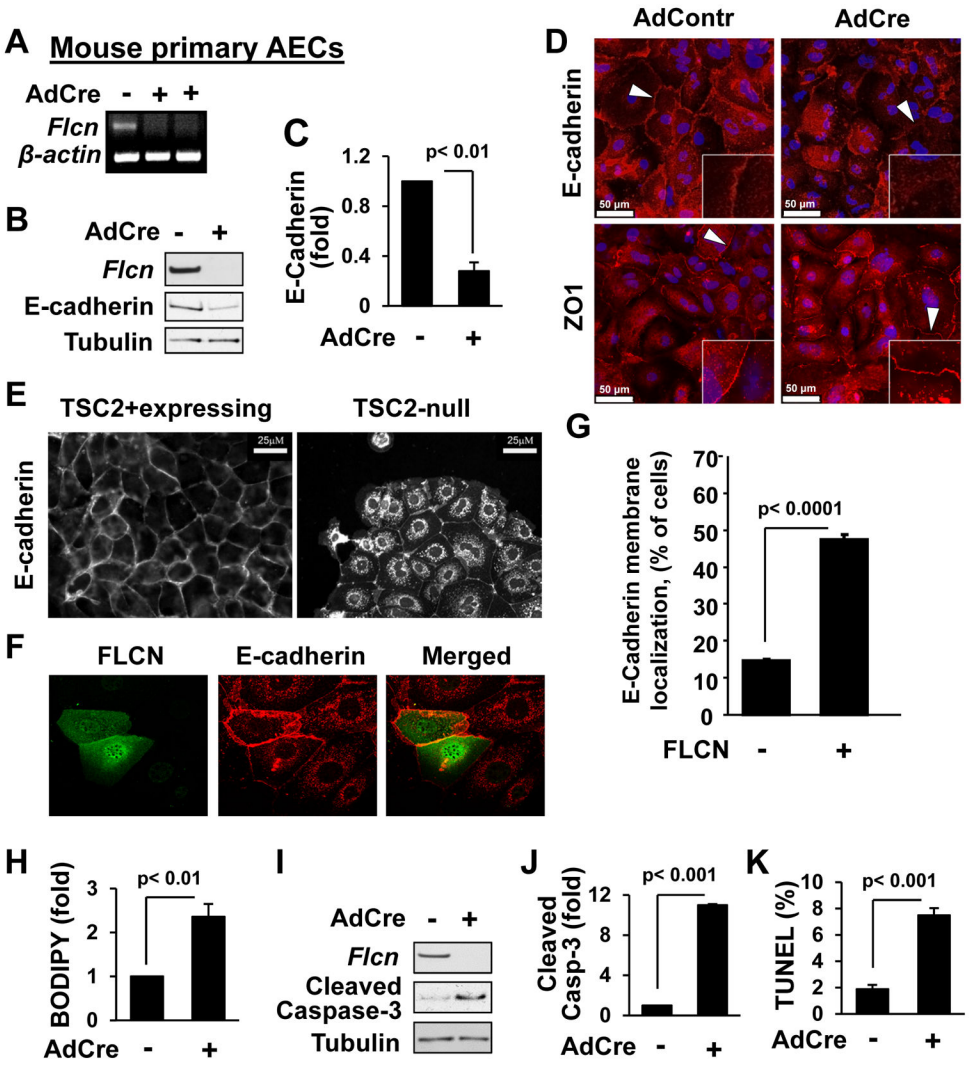

Figure 5. ***Flcn*** **loss reduces E-Cadherin levels, increases cellular permeability and promotes apoptosis of primary mouse lung AECs**

(A–C) AdCre-induced *Flcn* deletion in AECs from *Flcn*$^{f/f}$ mice was detected by RT-PCR (A) and immunoblot (B) with statistical analysis (C). E-cadherin/tubulin ratio for control cells is taken as one fold.

(D) Loss of FLCN in AECs downregulates membrane localization of E-Cadherin (red, upper panel) but not ZO1 (red, lower panel). DAPI (blue) stains nuclei. Scale bars, 50 μM. See also Figure S4.

(E) Cytoplasmic E-cadherin localization in *TSC2*-null epithelial cells. Scale bars, 25 μM.

(F–G) FLCN expression (green) results in membrane localization of E-cadherin (red) in TSC2-null cells (F). Data (G) represent % of cells, > 60 cells/condition (F).

(H) *Flcn* deletion increases lung AEC permeability. Cell permeability in control is taken as one fold.

(I–J) *Flcn* deletion in lung AECs upregulates cleaved caspase-3.

(K) *Flcn* deletion in AECs results in DNA fragmentation. Number of TUNEL-positive cells to total number of cells is taken as 100%.

Data are mean ± SE, n>3.

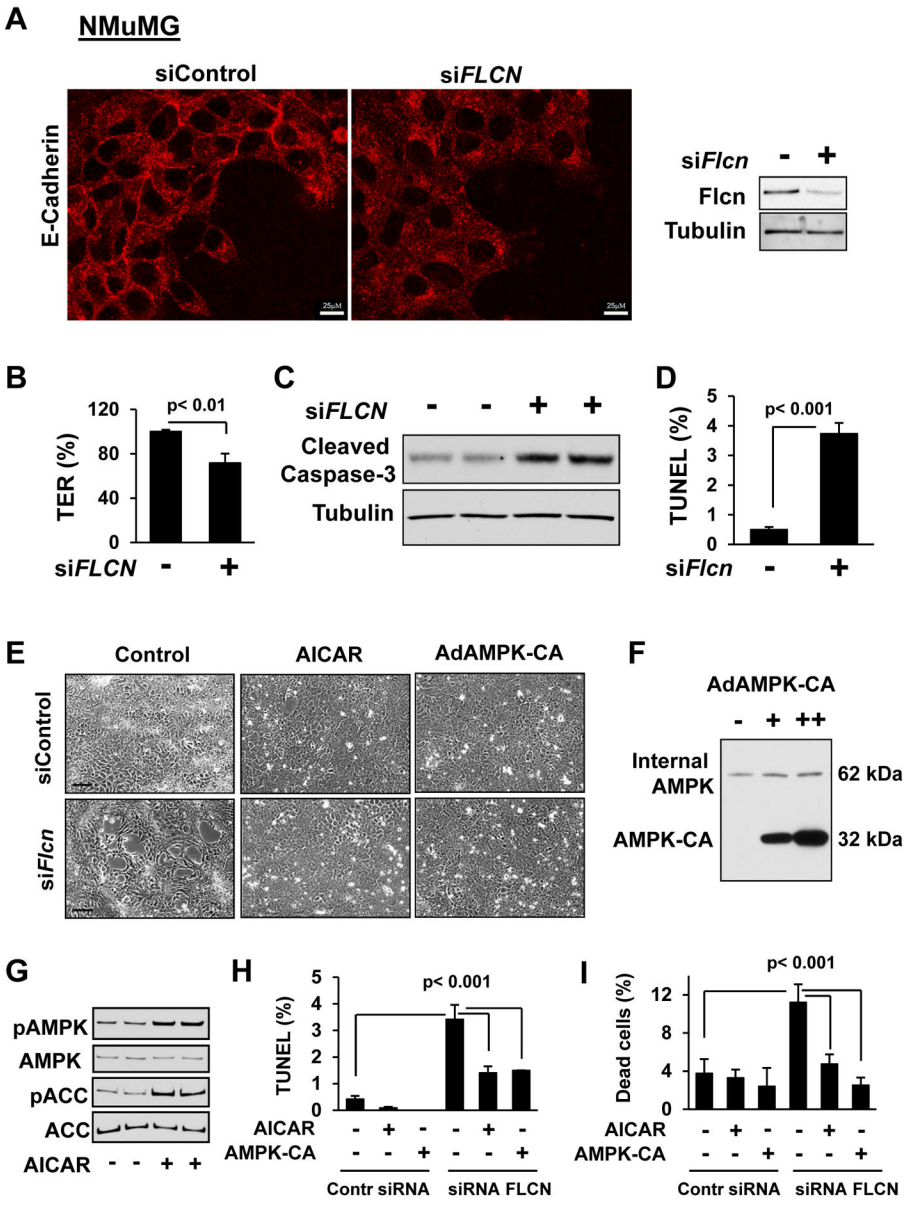

Figure 6. Increased *Flcn*-null epithelial cell apoptosis is rescued by AICAR and constitutively active AMPK

(A) Flcn knockdown downregulates membrane localization of E-cadherin (red). Scale bars, 25 μM.

See also Figure S5 and S6.

(B) Flcn knockdown decreases trans-epithelial resistance (TER). TER of siContr-transfected NMuMG cells was taken as 100%.

(C) Cleaved caspase-3 is upregulated by si*Flcn*.

(D) Flcn knockdown induces DNA fragmentation (TUNEL assay) of NMuMG cells.

(E) AICAR and constitutively active AMPK (AMPK-CA) rescue disruption of epithelial cell morphology caused by si*Flcn*. Cells were treated either with 100 mM AICAR or diluent, or were infected with AdAMPK-CA or control adenovirus. Scale bars, 100 μM.

(F–G) Expression of AMPK-CA (F) and AICAR-induced AMPK and ACC (G) phosphorylation in epithelial NMuMG cells.

(H–I) DNA fragmentation (H) and epithelial cell death (I) induced by Flcn loss is rescued by AICAR and AMPK-CA. Data represent percentage of TUNEL-positive (H) or dead (I) cells per total number of cells taken as 100%.

Data are mean ± SE, n=3.

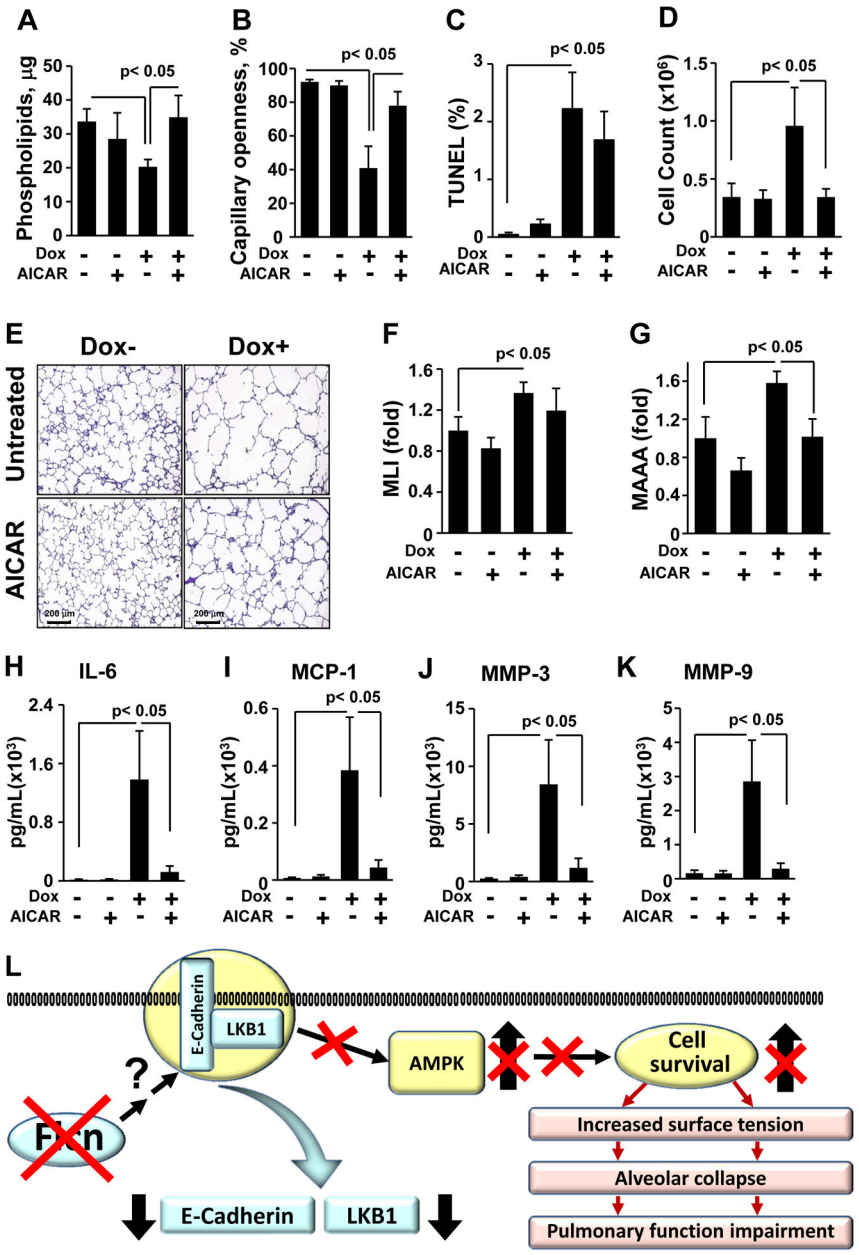

Figure 7. AICAR improves lung homeostasis of *Flcn*$^{f/f}$*:SP-C-Cre* mice with *Flcn* deletion in lung epithelium

(A) Abnormalities in pulmonary phospholipids in BAL resulting from *Flcn* deficiency are restored by AICAR. *Flcn*$^{f/f}$*:SP-C-Cre* mice on Dox- or Dox+ were treated with AICAR or diluent for 6 weeks.

(B) *Flcn*-induced impairment of surfactant surface tension is rescued by AICAR.

(C) *Flcn* loss induces DNA fragmentation of AECs. Number of TUNEL-positive cells to total number of cells was taken as 100%.

(D) AICAR normalizes increased inflammatory cell influx.

(E) H&E staining of *Flcn*$^{f/f}$*:SP-C-Cre* mouse lungs on Dox- or Dox+ treated with AICAR as in (A).

(F, G) Morphometric analyses of *Flcn*$^{f/f}$*:SP-C-Cre* mouse lungs treated as in (A). The mean is shown; error bars represent SE (n>3). Data for Dox- mice are taken as one fold.
(H, I) AICAR inhibits IL-6 (H) and MCP-1 (I) increased by *Flcn* loss.
(J, K) Upregulation of MMP-3 and MMP-9 induced by *Flcn* loss in lung epithelium treated as in (A) are abrogated by AICAR.
See also Figure S7.
Data (A-K) are represented as mean ± SEM from two independent experiments, n = 5–7.
(L) A proposed model for the role of FLCN in lung alveolar homeostasis. *FLCN* mutations in lung epithelium downregulate membrane localization of E-cadherin and LKB1 which impairs AMPK activation. This model proposes that FLCN plays an important physiological function to control alveolar epithelial cell survival and maintains alveolar surface tension. Loss of FLCN results in alveolar collapse and impairment of lung function.